Multiphase flow models in a network of pipes

Jean Medard T Ngnotchouye[1] MK Banda[2] M Herty[3]

[1]School of Mathematics, Statistics and Computer Sciences University of KwaZulu-Natal
[2]Department of mathematics, University of Pretoria [3]RWTH Aachen, Germany

Evolutionary processes on networks
Kigali, Rwanda, 20-24th March 2018

Outline

Multiphase flow networks for subsea oil and gas production

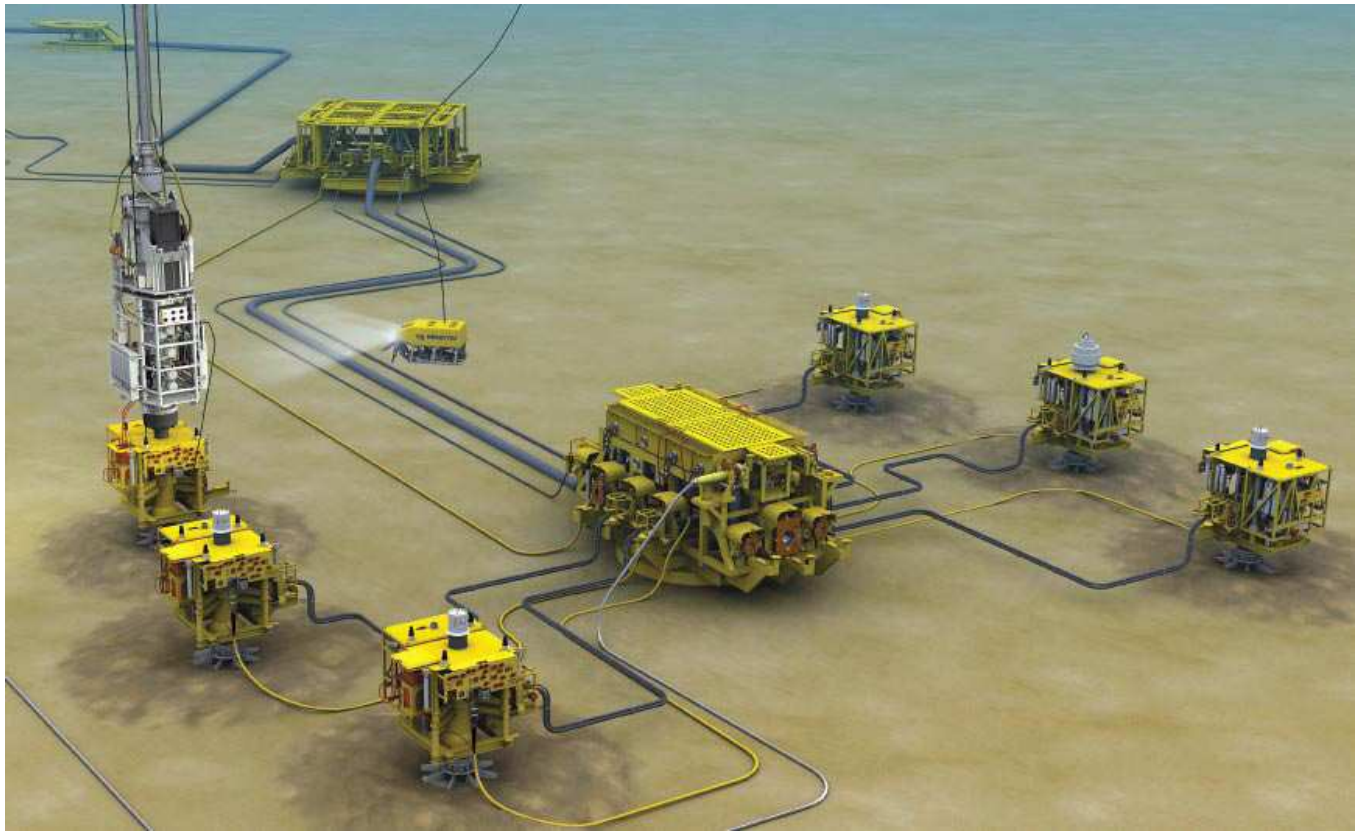

Multiphase flow networks for subsea oil and gas production

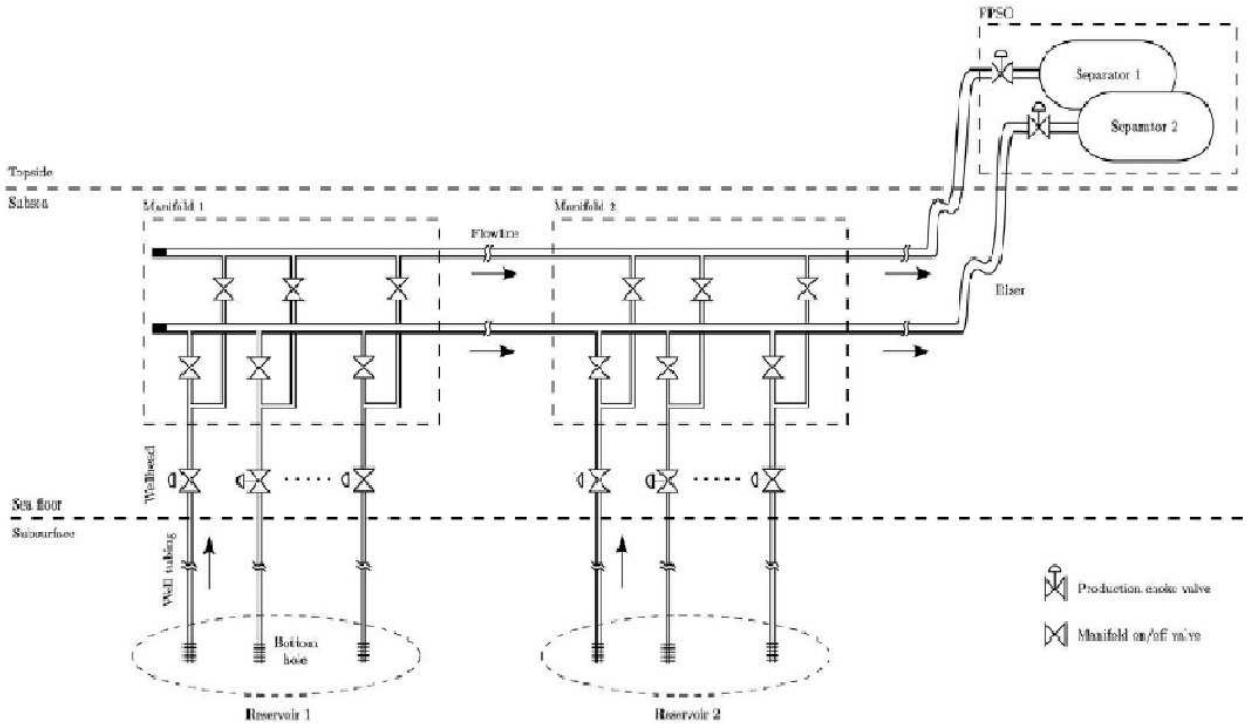

Multiphase flow networks for subsea oil and gas production

- In these networks, there is a presence of wells, collection systems, pipelines, processing units such as pumps and separators.
- Real time data capture and storage capabilities have paved the way for the use of model-based techniques to improve operations.
- In practice, the use of model-based methods translates into advisory systems for production engineers.
- Such systems use real-time data in combination with calibrated mathematical models and optimisation to improve the economics of an oil field by increasing throughput.
- Some claims to a production increase of up to 4% due to the use of model based tools
- Grimstad et al. [Grimstad et al., 2016] propose a global optimisation method using spline-based surrogate model.
- Their main strategies are to adapt well-known graph based modeling scheme to oil and gas network, then use spline-based surrogate models to represent the nonlinear parts of the system and then use a global branch

Steady state analysis of gas network with distributed injection of alternative gas

- Natural gas seem to be a viable alternative to curb high carbon emission by industrialized countries.
- Steady state analysis of gas networks is usually used to compute nodal pressures and pipe flows for given values of source node pressures and gas consumption.
- Traditional methods of modeling and simulating gas networks assume a gas mixture with a uniform composition to be transported via the network
- Abeysekera et al. [Abeysekera et al., 2016] propose methods for simulation of gas networks considering a diversity of alternative gas (hydrogen, upgraded biogas)injections.
- In their proposed method, a set of algebraic equations, equal in number to the state variables to be calculated are formulated using the gas pipe flow equations and Kirchhoffs first law applied at nodes.
- Injection of alternative gases in a gas grid has an impact both at appliance level and at network level.

Treating network junction in finite volume solution of transient flow

- For non-steady state flow in networks. Two main approaches have emerged in the literature: the coupling conditions at the junction and the coupling of 1D and 2D models at the junction.
- Bermúdez et al [Bermúdez et al., 2017] propose a finite volume method to solve the equations modelling the gas flow in gas transportation networks consisting of pipelines interconnected at nodes and some other elements like compression stations, pressure/flow control valves, underground storages, etc.
- The model is based on the Euler equation with a source term that account for pipe friction, pipe length and diameter.
- The approach of Bermúdez is a coupling of 1D and 2D models at the junctions.

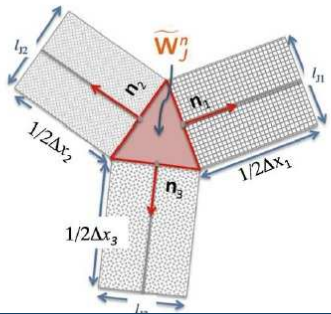

A review of multiphase models in networks

- In the past, analysis of two-phase flow pipelines in the petroleum industry were performed primarily with the use of steady-state methods.
- However, various operational events such as flow rate changes, shutdowns-restarts, and pipeline leaks cause unsteady flow. Clearly, steady-state methods can not be applied to perform analysis under these circumstances and transient two-phase flow calculations should be used.
- Multiphase flow is a phase in which natural gas is found in the process of oil recovery from the reservoir.
- The reservoir contains in general a large quantity of methane along with heavier hydrocarbons such as ethane, propane, isobutane, normal butane, etc.
- It is also generally saturated with water.

The drift-flux model

- We consider a non-isothermal transient two-phase model in a pipe with the assumptions that the amount of liquid is small and the gas flow rate is high with both the gas and liquid phases obeying the laws of continuum mechanics,
- the liquid droplet are assumed to have uniform size,
- the flow is assumed to be one-dimensional in the axial direction of the pipe and the diameter of the pipe is assumed to be constant along the pipe,
- gas and liquid phases are assumed to be at local equilibrium at every point within the pipe,
- dissipation and compression terms are neglected and there is no coagulation, nor agglomeration [Dukhovnaya and Adewumi, 2000].

Problem formulation

- The governing equations can be written in conservative form as

$$\frac{\partial U}{\partial t} + \frac{\partial f(U)}{\partial x} = G(U) \tag{1}$$

where

$$U = \begin{bmatrix} \rho_g \\ \rho_l \\ m_g \\ m_l \\ H_g \\ H_l \end{bmatrix}; \quad f(U) = \begin{bmatrix} m_g \\ m_l \\ \frac{m_g^2}{\rho_g} + c_g^2 \rho_g \\ \frac{m_l^2}{\rho_l} + c_l^2 \rho_l \\ H_g \frac{m_g}{\rho_g} \\ H_l \frac{m_l}{\rho_l} \end{bmatrix}; \quad G(U) = \begin{bmatrix} M_{gl} \\ M_{lg} \\ -\sum F_{i_g} - \alpha_g \varrho_g g \sin\theta \\ -\sum F_{i_l} - \alpha_l \varrho_l g \sin\theta \\ Q_g + h_{gl} + h_g \\ Q_l + h_{lg} + h_l \end{bmatrix} \tag{2}$$

Problem formulation

- These equations are derived from the continuity equations, the momentum equations and the energy equations under the assumptions that the rate of change of the volume fractions α_g and α_l with respect to the flow direction are sufficiently small and that the sound speeds c_g and c_l are constant along the flow direction.
- The conservative variables are related to the primal variable through the relationships

$$\begin{aligned} \rho_g &= \varrho_g \alpha_g & \rho_l &= \varrho_l \alpha_l, \\ m_g &= \varrho_g \alpha_g v_g & m_l &= \varrho_l \alpha_l v_l, \\ H_g &= \varrho_g \alpha_g \tilde{H}_g & H_l &= \varrho_l \alpha_l \tilde{H}_l. \end{aligned} \tag{3}$$

$\varrho_{g,l}$, $v_{g,l}$ and $\tilde{H}_{g,l}$ are the densities, velocity and enthalpy of the gas and liquid phases, respectively.

Problem formulation

- We note that the two phases fill the entire pipe:

$$\alpha_g + \alpha_l = 1.$$

- The mass transfer rate experienced by the gas and liquid phases are equal in magnitude but of opposite sign:

$$M_{gl} = -M_{lg}.$$

- The drag forces and mass transfer forces exerted on one phase by the other are equal but of opposite sign:

$$F_{dg} = -F_{dl}, \quad F_{mg} = -F_{ml}.$$

- The energy transfer rate from one phase to another are equal and the rate of change of latent heat from one phase to another are equal but of opposite sign:

$$h_{gl} = -h_{lg}, \quad h_g = -hl.$$

Problem formulation

- The frictional force between each phase and the pipe wall is determined using volume-fraction-modified form of the single phase flow model. The mixture properties in the single-phase model are replaced with the phasic properties. For gas and liquid phases the frictional forces are written as:

$$F_{wg} = \frac{\alpha_g f_g \varrho_g v_g |v_g|}{2d}$$
$$F_{wl} = \frac{\alpha_l f_l \varrho_l v_l |v_l|}{2d}$$

- where f_g and f_l are Darcy's friction factors for gas and liquid phases, respectively. These are calculated using Chen's equation

An hierarchy of models related to the drift-flux model

- Following [Domschke et al., 2018] we define an hierachy of models derived from the drift-flux model
- For the first simplified model, we assume that the velocity and pressure of the two phases are equal and that the source term is zero. We then obtain the no-slip drift-flux model [Banda et al., 2010b]in conservative form

$$\begin{aligned} \partial_t \rho_1 + \partial_x \frac{\rho_1 I}{\hat{\rho}} &= 0; \\ \partial_t \rho_2 + \partial_x \frac{\rho_2 I}{\hat{\rho}} &= 0; \\ \partial_t I + \partial_x \left(\hat{\rho}(u^2 + \frac{a^2}{2}) \right) &= 0; \end{aligned} \tag{4}$$

where $\hat{\rho} = \rho_1 + \rho_2$, $I = \hat{\rho} u$.

An hierarchy of models related to the drift-flux model

- At the next approximation, we assume that the sonic speed of the two phases are different. This gives the simplified model [Banda et al., 2010a]

$$\begin{cases} \partial_t \rho_1 + \partial_x \frac{\rho_1 I}{\hat{\rho}} &= 0 \\ \partial_t \rho_2 + \partial_x \frac{\rho_2 I}{\hat{\rho}} &= 0 \\ \partial_t I + \partial_x \left(\frac{I^2}{\hat{\rho}} + \rho_1 a_1^2 + \rho_2 a_2^2 \right) &= 0 \end{cases} \tag{5}$$

  where we have taken $I = \hat{\rho} u$, $\hat{\rho} = \rho_1 + \rho_2$.

- At the next level, we assume that the pressure $p(\rho_1, \rho_2)$ is as general as possible.

- This model was analyzed in [Banda et al., 2015] using the idea of linearisation of the Lax curve.

The corresponding conservation law problem

- The equation (1) can be written in quasi-linear form as

$$U_t + A(U)U_x = H(U), \tag{6}$$

where $A(U)$ is the Jacobian matrix of the flux function f evaluated as

$$A(U) = \begin{bmatrix} 0 & 0 & 1 & 0 & 0 & 0 \\ 0 & 0 & 0 & 1 & 0 & 0 \\ c_g^2 - v_g^2 & 0 & 2v_g^2 & 0 & 0 & 0 \\ 0 & c_l^2 - v_l^2 & 0 & 2v_l^2 & 0 & 0 \\ -v_g H_g & 0 & H_g & 0 & v_g & 0 \\ 0 & -v_l H_l & 0 & H_l & 0 & v_l \end{bmatrix}$$

Problem formulation

- The eigenvalues of matrix $A(U)$ are:

$$\begin{array}{lll} \lambda_1 = v_g - c_g; & \lambda_2 = v_g; & \lambda_3 = v_g + c_g; \\ \lambda_4 = v_l - c_l; & \lambda_5 = v_l; & \lambda_6 = v_l + c_l. \end{array} \tag{7}$$

- with the corresponding right eigenvectors

$$r_1 = \begin{bmatrix} 1 \\ 0 \\ v_g - c_g \\ 0 \\ H_g \\ 0 \end{bmatrix}; \quad r_2 = \begin{bmatrix} 0 \\ 0 \\ 0 \\ 0 \\ H_g \\ 0 \end{bmatrix}; \quad r_3 = \begin{bmatrix} 1 \\ 0 \\ v_g + c_g \\ 0 \\ H_g \\ 0 \end{bmatrix}; \tag{8}$$

Problem formulation

- and

$$r_4 = \begin{bmatrix} 0 \\ 1 \\ 0 \\ v_l - c_l \\ 0 \\ H_l \end{bmatrix}; \quad r_5 = \begin{bmatrix} 0 \\ 0 \\ 0 \\ 0 \\ 0 \\ H_l \end{bmatrix} \quad r_6 = \begin{bmatrix} 0 \\ 1 \\ 0 \\ v_l + c_l \\ 0 \\ H_l \end{bmatrix}. \tag{9}$$

The Riemann problem

- We have

$$\nabla\lambda_1\, r_1 = -\frac{c_g}{\rho_g}; \quad \nabla\lambda_2\, r_2 = 0; \quad \nabla\lambda_3\, r_3 = \frac{c_g}{\rho_g};$$
$$\nabla\lambda_4\, r_4 = -\frac{c_l}{\rho_l}; \quad \nabla\lambda_5\, r_5 = 0; \quad \lambda_6\, r_6 = \frac{c_l}{\rho_l}.$$

- Hence the fields 1,3,4 and 6 are genuinely non linear while the fields 2 and 5 are linearly degenerate.
- From standard result on conservation laws, see for example [Dafermos, 2005, Bressan, 2000], the associated Cauchy problem and hence the Riemann problem has a solution.

The Riemann problem

- We have

$$\nabla\lambda_1\, r_1 = -\frac{c_g}{\rho_g}; \quad \nabla\lambda_2\, r_2 = 0; \quad \nabla\lambda_3\, r_3 = \frac{c_g}{\rho_g};$$
$$\nabla\lambda_4\, r_4 = -\frac{c_l}{\rho_l}; \quad \nabla\lambda_5\, r_5 = 0; \quad \lambda_6\, r_6 = \frac{c_l}{\rho_l}.$$

- Hence the fields 1,3,4 and 6 are genuinely non linear while the fields 2 and 5 are linearly degenerate.
- From standard result on conservation laws, see for example [Dafermos, 2005, Bressan, 2000], the associated Cauchy problem and hence the Riemann problem has a solution.

The Riemann problem

- The (standard) Riemann problem consist of solving the model equation with heaviside type initial condition, namely

$$U(0,x) = \begin{cases} U_l & x < 0, \\ U_r & x > 0, \end{cases} \tag{10}$$

where U_l and U_r are fixed states in $\mathbb{R}^6$.

- As it is well known, see [Bressan, 2000], the solution is a juxtaposition of fixed states separated by wave curves.
- The Hugoniot locus of a fixed state $\bar{U} = (\bar{\rho}_g, \bar{\rho}_l, \bar{m}_g, \bar{m}_l, \bar{H}_g, \bar{H}_l)$ is the set of states $U = (\rho_g, \rho_l, m_g, m_l, H_g, H_l)$ that can be connected to $\bar{U}$ through a jump satisfying the Rankine-Hugoniot jump conditions

$$f(U) - f(\bar{U}) = s(U - \bar{U}),$$

where s is called the shock speed.

The Riemann problem

- This gives the system of equations

$$
\begin{aligned}
m_g - \bar{m}_g &= s(\rho_g - \bar{\rho}_g), && (11)\\
m_l - \bar{m}_l &= s(\rho_l - \bar{\rho}_l), && (12)\\
\frac{m_g^2}{\rho_g} + c_g^2\rho_g - \frac{\bar{m}_g^2}{\bar{\rho}_g} - c_g^2\bar{\rho}_g &= s(m_g - \bar{m}_g), && (13)\\
\frac{m_l^2}{\rho_l} + c_l^2\rho_l - \frac{\bar{m}_l^2}{\bar{\rho}_l} - c_l^2\bar{\rho}_l &= s(m_l - \bar{m}_l), && (14)\\
H_g\frac{m_g}{\rho_g} - \bar{H}_g\frac{\bar{m}_g}{\bar{\rho}_g} &= s(H_g - \bar{H}_g), && (15)\\
H_l\frac{m_l}{\rho_l} - \bar{H}_l\frac{\bar{m}_l}{\bar{\rho}_l} &= s(H_l - \bar{H}_l). && (16)
\end{aligned}
$$

- This is a system of six equations with seven unknowns.

The Riemann problem

- Solving for the variables ρ_l, m_g, m_l, H_g, H_l and s in terms of ρ_g gives the 1-3 shock curves as

$$S_{1,3}(\xi;\bar{U}):\xi\mapsto\begin{bmatrix}\bar{\rho}_g\xi\\ \frac{\bar{\rho}_l}{c_l^2}\left(\frac{\bar{m}_g}{\bar{\rho}_g}-\frac{\bar{m}_l}{\bar{\rho}_l}\mp c_g\sqrt{\xi}\right)^2\\ \bar{m}_g\xi\mp c_g\bar{\rho}_g\sqrt{\xi}(\xi-1)\\ \bar{m}_l+\left(\frac{\bar{m}_g}{\bar{\rho}_g}\mp c_g\sqrt{\xi}\right)\left[\frac{\bar{\rho}_l}{c_l^2}\left(\frac{\bar{m}_g}{\bar{\rho}_g}-\frac{\bar{m}_l}{\bar{\rho}_l}\mp c_g\sqrt{\xi}\right)^2-\bar{\rho}_l\right]\\ \bar{H}_g\xi\\ \bar{H}_l\frac{\frac{\bar{m}_l}{\bar{\rho}_l}-\frac{\bar{m}_g}{\bar{\rho}_g}\pm c_g\sqrt{\xi}}{\frac{m_l}{\rho_l}-\frac{\bar{m}_g}{\bar{\rho}_g}\pm cg\sqrt{\xi}}\end{bmatrix}. \tag{17}$$

- The shock speeds associated with the 1 and 3-fields are

$$s_{1,3}=\frac{\bar{m}_g}{\bar{\rho}_g}\mp c_g\sqrt{\frac{\rho_g}{\bar{\rho}_g}}. \tag{18}$$

The Riemann problem

- Similarly, the 4-6 shock curves can also be found as

$$S_{4,6}(\xi;\bar{U}):\xi\mapsto\begin{bmatrix}\frac{\bar{\rho}_g}{c_g^2}\left(\frac{\bar{m}_l}{\bar{\rho}_l}-\frac{\bar{m}_g}{\bar{\rho}_g}\mp c_l\sqrt{\xi}\right)^2\\ \bar{\rho}_l\xi\\ \bar{m}_g+\left(\frac{\bar{m}_l}{\bar{\rho}_l}\mp c_l\sqrt{\xi}\right)\left[\frac{\bar{\rho}_g}{c_g^2}\left(\frac{\bar{m}_l}{\bar{\rho}_l}-\frac{\bar{m}_g}{\bar{\rho}_g}\mp c_l\sqrt{\xi}\right)^2-\bar{\rho}_g\right]\\ \bar{m}_l\xi\mp c_l\bar{\rho}_l\sqrt{\xi}(\xi-1)\\ \bar{H}_g\frac{\frac{\bar{m}_g}{\bar{\rho}_g}-\frac{\bar{m}_l}{\bar{\rho}_l}\pm c_l\sqrt{\xi}}{\frac{m_g}{\rho_g}-\frac{\bar{m}_g}{\bar{\rho}_g}\pm cg\sqrt{\xi}}\\ \bar{H}_l\xi\end{bmatrix}. \tag{19}$$

- with the corresponding shock speed as

$$s_{4,6}=\frac{\bar{m}_l}{\bar{\rho}_l}\mp\left|\frac{\bar{m}_g}{\bar{\rho}_g}\mp c_g\sqrt{\frac{\rho_g}{\bar{\rho}_g}}-\frac{\bar{m}_l}{\bar{\rho}_l}\right|. \tag{20}$$

The Riemann problem

- The admissible, in the sense of Lax, forward 1,4-shock and 3,6-shock waves satisfy $\xi > 1$ and $\xi < 1$, respectively while the backward shock waves satisfy the reverses inequalities.
- The rarefaction curves are found as the integral curves of the eigenvectors of the flux function.
- Their expression are found by solving the ordinary differential equation

$$\frac{d}{d\tau} U = \frac{r_i(U)}{\nabla \lambda_i(U) \cdot r_i(U)}, \quad U(0) = \bar{U}. \tag{21}$$

- The solution of the ODE (21) gives the 1 and 3-rarefaction curves as

$$R_1(\xi; \bar{U}) : \xi \mapsto \begin{bmatrix} \bar{\rho}_g \xi \\ \bar{\rho}_l \\ (\bar{m}_g - c_g \bar{\rho}_g \ln \xi)\xi \\ \bar{m}_l \\ \bar{H}_g \xi \\ \bar{H}_l \end{bmatrix}; \quad R_3(\xi; \bar{U}) : \xi \mapsto \begin{bmatrix} \bar{\rho}_g \xi \\ \bar{\rho}_l \\ (\bar{m}_g + c_g \bar{\rho}_g \ln \xi)\xi \\ \bar{m}_l \\ \bar{H}_g \xi \\ \bar{H}_l \end{bmatrix}. \tag{22}$$

The Riemann problem

- Similarly, the 4 and 6 -rarefaction curves are given by

$$R_4(\xi;\bar{U}):\xi\mapsto\begin{bmatrix}\bar{\rho}_g\\ \bar{\rho}_l\xi\\ \bar{m}_g\\ (\bar{m}_l-c_l\bar{\rho}_l\ln\xi)\xi\\ \bar{H}_g\\ \bar{H}_l\xi\end{bmatrix};\quad R_6(\xi;\bar{U}):\xi\mapsto\begin{bmatrix}\bar{\rho}_g\\ \bar{\rho}_l\xi\\ \bar{m}_g\\ (\bar{m}_l+c_l\bar{\rho}_l\ln\xi)\xi\\ \bar{H}_g\\ \bar{H}_l\xi\end{bmatrix}. \tag{23}$$

- Along the contact discontinuities, only the enthalpy changes and we obtain the contact discontinuity wave curves as

$$L_2(\xi;\bar{U}):\xi\mapsto\begin{bmatrix}\bar{\rho}_g\\ \bar{\rho}_l\\ \bar{m}_g\\ \bar{m}_l\\ \frac{\bar{H}_g}{\bar{\rho}_g}\xi\\ \bar{H}_l\end{bmatrix};\quad L_5(\xi;\bar{U}):\xi\mapsto\begin{bmatrix}\bar{\rho}_g\\ \bar{\rho}_l\\ \bar{m}_g\\ \bar{m}_l\\ \bar{H}_g\\ \frac{\bar{H}_l}{\bar{\rho}_l}\xi\end{bmatrix}. \tag{24}$$

The Riemann problem

- A typical solution to the Riemann problem has the wave structure depicted in the figure below

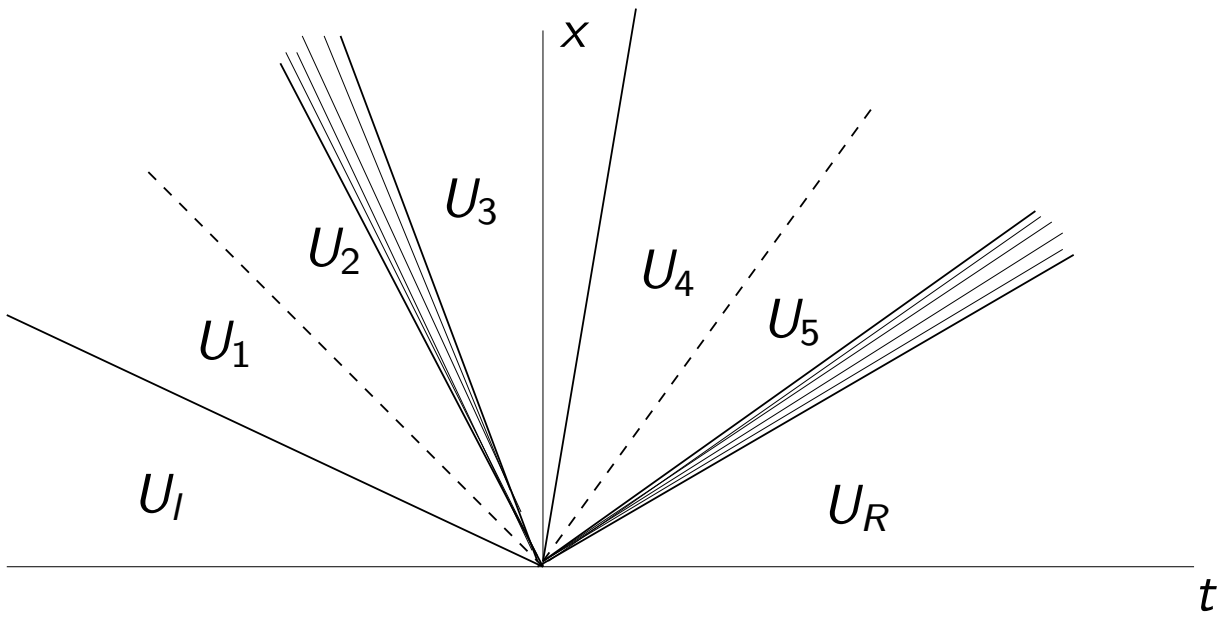

Figure: A typical solution to the standard Riemann problem

- therein, the dotted line represent a contact discontinuity curve, the fan represent the rarefaction curve and the thick solid line represent a shock curve.

The Riemann problem

- In this case the intermediary states are worked out as

$$\begin{array}{lll} U_1 = L_1^+(\xi_1, U_l), & U_2 = L_2(\xi_2, U_1), & U_3 = L_3^+(\xi_3, U_2), \\ U_4 = L_4^+(\xi_4, U_3), & U_5 = L_5(\xi_5, U_4), & U_6 = L_6^+(\xi_6, U_5). \end{array} \tag{25}$$

- The parameter $\xi = (\xi_1, \xi_2, \xi_3, \xi_4, \xi_5, \xi_6)$ are obtained by solving the equation

$$U_6 - U_r = 0 \tag{26}$$

  for ξ.

- We solve below this nonlinear equation numerically using the Newton's method.

The Riemann problem

- We depict below a projection of the forward 1,3-waves curves in the $\rho_g - m_g$ plane and the projection of the forward 4-6 wave curves in the $\rho_l - m_l$ plane for a fixed state

$$\bar{U} = \begin{bmatrix} 1.0 & 0.11 & 2.5 & 1.2 & 45.0 & 11.0 \end{bmatrix}^T.$$

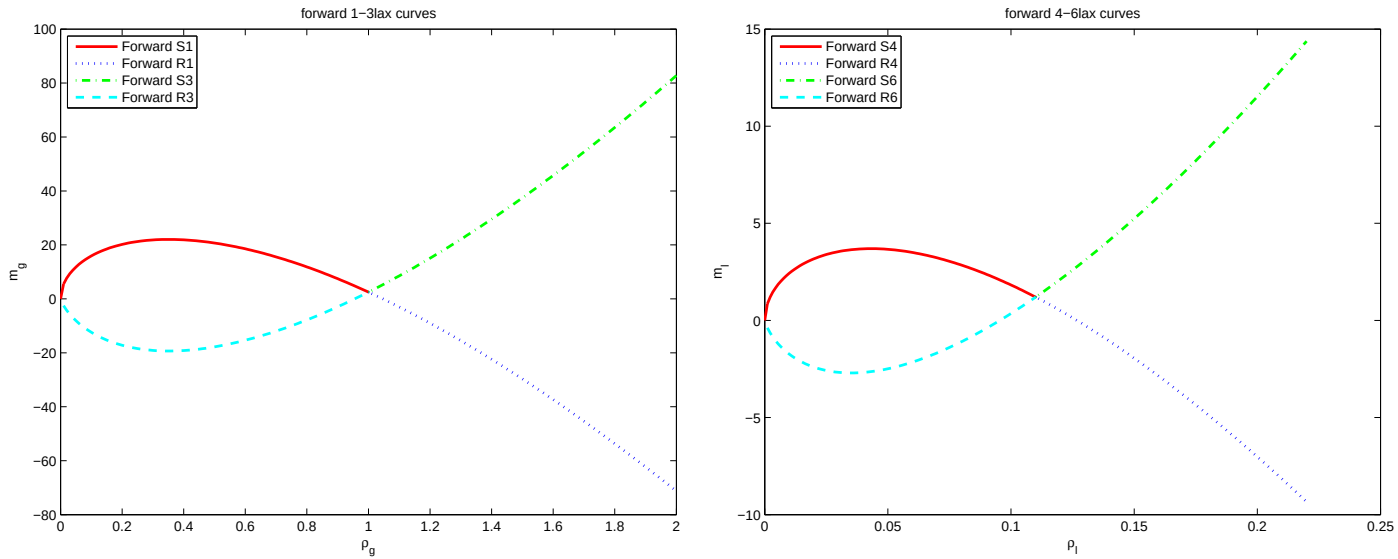

Figure: 1,3-forward Lax curves for the multiphase model in the $\rho_g - m_g$ plane (left) and 4,6-forward Lax curves for the multiphase model in the $\rho_l - m_l$ plane.

The Riemann problem

Theorem[Bressan, 2000]

For $\|U_r - U_l\|$ sufficiently small, there exists a unique self similar solution to the Riemann problem (1,10) with small total variation. The solution comprises 7 constant states $U_0 = U_l$, $U_1, \ldots, U_6 = U^r$. When the i-th characteristic field is linearly degenerate, U_i is joined to U_{i-1} by an i-contact discontinuity curve, while when the i-characteristic field is genuinely nonlinear, U_i is joined to U_{i-1} by either an i-(Lax) rarefaction or an i-(Lax) shock curve.

A Numerical example

- We consider an example where the Riemann problem is solved exactly as in Theorem above. We will describe the qualitative behavior of the solution by writing for example $\mathcal{S}_1 - \mathcal{C}_2 - \mathcal{R}_3 - \mathcal{S}_4 - \mathcal{C}_5 - \mathcal{S}_6$ to signify that the solution has a shock wave in the $1-$field, a contact discontinuity in the $2-$field, a rarefaction wave in the $3-$field, a shock wave in the $4-$field, a contact discontinuity in the $5-$field and a shock wave in the $6-$field.
- In the first example we consider a multiphase flow with the sound speeds $c_g = 30.5000$ and $c_l = 100.5$

A Numerical example

- The initial conditions are given in the table below. Note that in this example the mixture is at rest at the initial time on both sides of the membrane.

	ρ_g	ρ_l	m_g	m_l	H_g	H_l
U_l	15.5000	1.0000	0.0000	0.0000	5.0000	11.0000
U_r	10.6000	1.1000	0.000	0.000	4.0000	10.8000

The intermediary states are presented in the next slide. The qualitative behavior of the solution is of the form $\mathcal{S}_1 - \mathcal{C}_2 - \mathcal{S}_3 - \mathcal{S}_4 - \mathcal{C}_5 - \mathcal{R}_6$.

A Numerical example

- Solution of the previous example

	ρ_g	ρ_l	m_g	m_l	H_g	H_l
U_l	15.5000	1.0000	0.0000	0.0000	5.0000	11.0000
U_1	80.6	0.5	-4528.9	36.2	26.0	5.3
U_2	80.6	0.5	-4528.9	36.2	30.4	5.3
U_3	64.6	0.5	-4.0668	35.1	24.4	5.7
U_4	10.6000	1.0498	0.00	-4.9250	4.0000	11.5482
U_5	10.6000	1.0498	0.00	-4.9250	4.0000	10.3075
U_r	10.6000	1.1000	0.0000	0.0000	4.0000	10.8000

A model for the network of pipes

- The network of pipes is considered as a oriented graph $(\mathcal{P}, \mathcal{V})$ where the edges $\mathcal{P}$ of the graph represent the pipes and the nodes $\mathcal{V}$ represent the junctions.
- Each pipe $j \in \mathcal{P}$ is parametrised by an interval $I_j \doteq [x_j^a, x_j^b]$.
- Each node of the graph correspond to a junction of pipes. For $v \in \mathcal{V}$, the set of pipe $j \in \mathcal{P}$ ingoing to v are denoted as δ_v^- and the set of outgoing pipes are denoted as δ_v^+.
- The set of all the pipes meeting at the junction v is denoted as $\delta_v = \delta_v^- \cup \delta_v^+$. We will call the cardinality of the set δ_v the degree of the junction v.

A model for the network of pipes

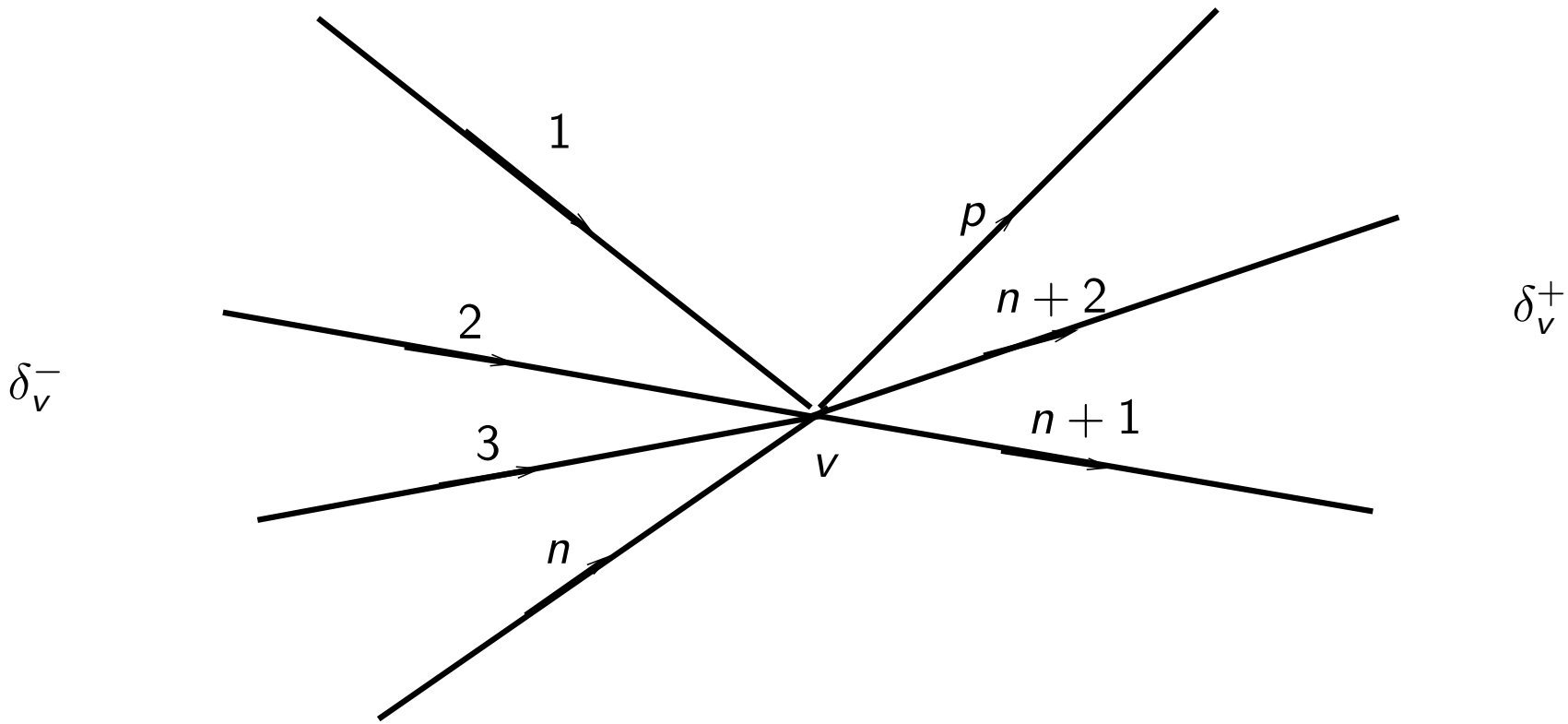

Figure: A junction with n ingoing pipes and $p - n$ outgoing pipes.

A model for the flow in a network of pipes

- We assume that for each pipe $j \in \mathcal{P}$, the flow is governed by the equation (4) rewritten as

$$\frac{\partial U^j}{\partial t} + \frac{\partial f(U^j)}{\partial x} = 0, \; U^j = \begin{bmatrix} \rho_1^j \\ \rho_2^j \\ I^j \end{bmatrix}, \tag{27}$$

  where the flux function is given either by (1), (4) or (5).

- The Riemann problem at the junction assumed for the analysis at $v = 0$ consists of solving the flow equations in all the pipes $j \in \delta_v$ with constant initial data in each pipe

$$U^j(0^{\pm}, x) = \tilde{U}^j, \; x_a^j \leq x \leq x_b^j, \tag{28}$$

  and with some coupling conditions at the junction v describing the interaction of the flow at the junction. These coupling conditions provide for the simulations as boundary conditions at the interior nodes of each pipe.

Coupling conditions at a junction

- For simplicity we consider the case of a junction with only two pipes, one ingoing and one outgoing. The result can be extended to junctions with higher degree in a straightforward way.
- At the junction, located at $x = 0$, the dynamics are governed by the coupling conditions

$$\Psi\left(w^-(t, 0-); w^+(t, 0+)\right) = 0, \tag{29}$$

where the w^- and w^+ are the flow variables in the left and right pipe, respectively.

- The subsonic region is defined as

$$A_0 = \{w \in \overset{\circ}{\mathbb{R}}^+ \times \overset{\circ}{\mathbb{R}}^+ \times \mathbb{R} : \lambda_1(w) < 0 < \lambda_2(w) < \lambda_3(w)\}. \tag{30}$$

- For later use, we define the quantities

$$M(w) = \frac{\rho_1 I}{\rho_1 + \rho_2}, \quad N(w) = \frac{\rho_2 I}{\rho_1 + \rho_2}, \quad P(w) = \frac{I^2}{\rho_1 + \rho_2} + p(\rho_1, \rho_2). \tag{31}$$

Coupling conditions at a junction

- We define the map

$$\hat{w}(x) = \begin{cases} \hat{w}^-, & \text{if } x < 0; \\ \hat{w}^+, & \text{if } x > 0; \end{cases} \quad \text{with} \quad \begin{array}{l} \Psi(\hat{w}^-; \hat{w}^+) = 0, \\ \hat{w}^-,\ \hat{w}^+ \in A_0 \end{array} \tag{32}$$

- A weak Ψ-solution of (4) complemented by (29) is a map

$$\begin{gathered} w \in \mathbf{C}^0\left(\mathbb{R}^+; \hat{w} + \mathbf{L}^1(\mathbb{R}; \overset{\circ}{\mathbb{R}}^+ \times \overset{\circ}{\mathbb{R}}^+ \times \mathbb{R})\right) \\ w(t) = w(t,\cdot) \in \mathbf{BV}(\mathbb{R}; \overset{\circ}{\mathbb{R}}^+ \times \overset{\circ}{\mathbb{R}}^+ \times \mathbb{R}) \quad \text{for a.e. } t \in \mathbb{R}^+ \end{gathered} \tag{33}$$

  such that

- for all $\varphi \in \mathbf{C}_c^1\left(\overset{\circ}{\mathbb{R}}^+ \times \mathbb{R}; \mathbb{R}\right)$ whose support does not intersect $x = 0$

$$\int_{\mathbb{R}^+}\int_{\mathbb{R}} \left(\begin{bmatrix} \rho_1 \\ \rho_2 \\ I \end{bmatrix} \partial_t \varphi + \begin{bmatrix} \frac{\rho_1 I}{\hat{\rho}} \\ \frac{\rho_1 I}{\hat{\rho}} \\ P(w) \end{bmatrix} \partial_x \varphi \right) dxdt = 0; \tag{34}$$

- for a.e. $t \in \mathbb{R}^+$, the junction condition is fulfilled

$$\Psi(w^-(t,0-); w^+(t,0+)) = 0.$$

Coupling conditions at a junction

- Consider now the coupling conditions

$$\Psi\left(w^{-};w^{+}\right)=\begin{bmatrix} M(w^{+})-M(w^{-}) \\ N(w^{+})-N(w^{-}) \\ P(w^{+})-P(w^{-}) \end{bmatrix}. \tag{35}$$

- This amounts to the conservation of mass of each phase and the equality of the dynamic pressure at the junction.
- It can be shown that using (35) a solution is equivalent to the classical solution of the Riemann problem on $\mathbb{R}$ with initial data in a neighborhood of a subsonic state $\bar{w}$.
- In general, the existence of the solution to the Riemann problem at the junction is proven by exhibiting some intermediary states that couples the flow at the junction though the Lax curves.

Coupling conditions at a junction

- For a junction with m ingoing pipes and p outgoing pipes with the flow variables in those pipes denoted by $w_j,\ j = 1, \dots m+p$, we adopt the following coupling condition map

$$\Psi(w_1, \dots, w_m, w_{m+1}, \dots, w_{m+p}) =$$

$$\begin{pmatrix}
\sum_{i=1}^{m} M(w_i(t,0-)) & = & \sum_{i=1}^{p} M(w_{m+i}(t,0+)) \\
\sum_{i=1}^{m} N(w_i(t,0-)) & = & \sum_{i=1}^{p} N(w_{m+i}(t,0+)) \\
P(w_1(t,0-)) & = & P(w_2(t,0-)) \\
 & \vdots & \\
P(w_{m-1}(t,0-)) & = & P(w_m(t,0-)) \\
P(w_m(t,0-)) & = & P(w_{m+1}(t,0+)) \\
P(w_{m+1}(t,0+)) & = & P(w_{m+2}(t,0+)) \\
 & \vdots & \\
P(w_{m+p-1}(t,0+)) & = & P(w_{m+p}(t,0+))
\end{pmatrix}.$$

Two connected pipes and the standard Riemann problem

- Here we verify the qualitative behavior of the coupling conditions and validate the use of the linearized Lax curves for a junction connecting two pipes.
- To achieve that goal, we use isothermal pressure law which is the same as the isentropic pressure law for $\gamma = 1$
- Independently, the standard Riemann problem, the Riemann problem at the junction with two horizontal pipes and with the exact Lax curves and then with the linearized Lax curves is solved. It is expected that the three results will agree.
- The choice of the isothermal pressure law for this test is motivated by the fact that the exact expressions for the Lax curves can be determined.
- Here the Riemann data is taken as

$$\begin{array}{l} w_l = (1.4712300, 2.2832400, 3.2928117), \\ w_r = (0.8070800, 1.2525284, 2.2928117) \end{array} . \tag{36}$$

- For the Riemann problem at the junction, $w_1 = w_l$ and $w_2 = w_r$ and the coupling conditions ar satisfied.

Two connected pipes and the standard Riemann problem

- r^{RP} is the quantity r computed as the solution of the standard Riemann problem and r^{CP} be the same quantity computed as the solution of the Riemann problem at the junction of two coupled pipes.

Mesh size (N)	$\|l^{RP} - l^{CP}\|_{L^2}$	$\|p^{RP} - p^{CP}\|_{L^2}$	$\|l^{RP} - l^{CP}\|_{L^2}$
100	1.6339e-06	1.8844e-06	0.0012
200	3.7917e-07	2.7096e-07	5.9362e-04
400	8.5111e-08	5.1969e-08	3.0193e-04

Table: L^2 error in the momentum and pressure for the solution of the standard Riemann problem and the Riemann problem at the junction

Two connected pipes and the standard Riemann problem

- Now an example with the isentropic pressure law is considered. Here $\gamma = 5/3$ is used and the following data

$$w_1 = (1.81832, 1.44174, -0.751082), \quad w_2 = (2.01667, 1.22004, -1.584711) \tag{37}$$

Mesh size (N)	$\|I^{CP} - I^{CPL}\|_{L^2}$	$\|p^{CP} - p^{CPL}\|_{L^2}$	$\|I^{CP} - I^{CPL}\|_{L^2}$
100	1.2886e-05	5.4828e-06	0.0038
200	3.0500e-06	1.2959e-06	0.0011
400	1.0113e-06	4.3049e-07	0.0012

Table: L^2 error in the momentum and pressure for the solution of the Riemann problem at the junction with exact Lax curves and linearised Lax curves computed for the problem in example 1

Two connected pipes and the standard Riemann problem

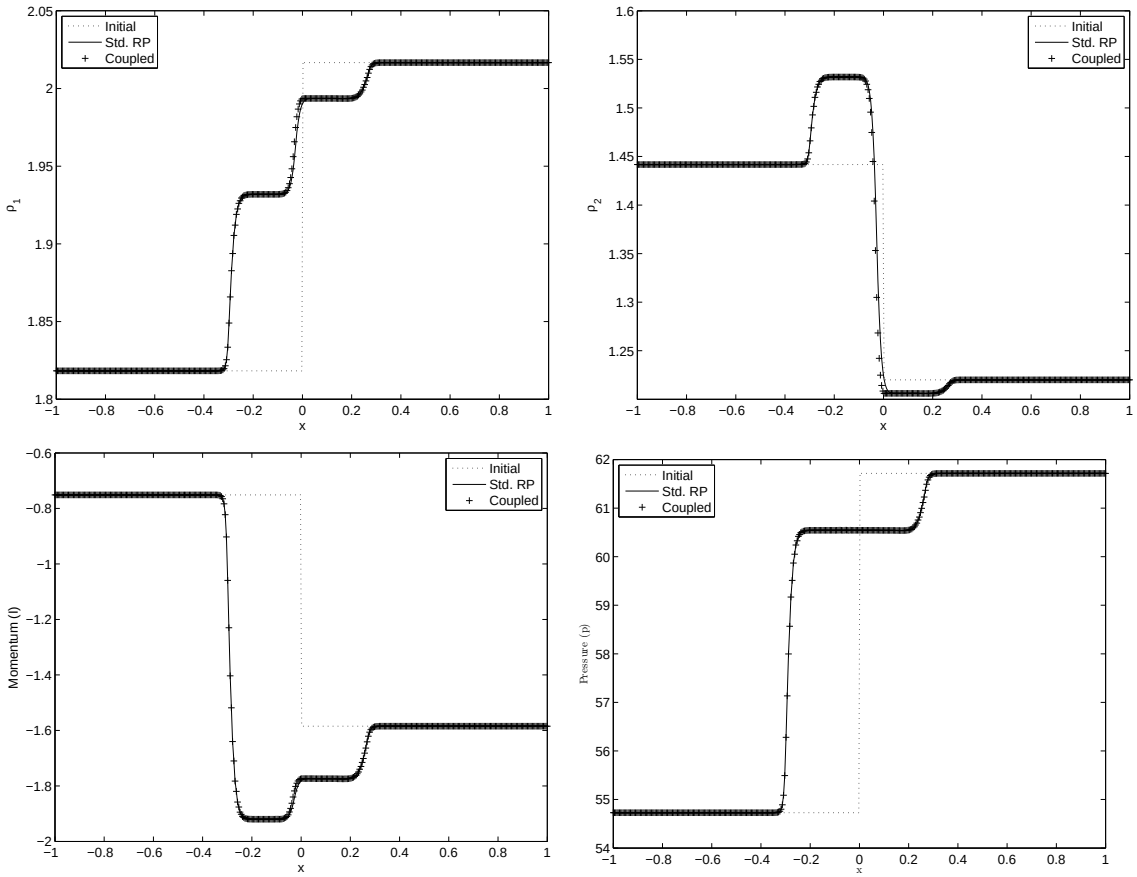

Figure: Profiles of the densities ρ_1 and ρ_2, the momentum I, the common pressure p for the solution of standard Riemann problem (continuous line) and the Riemann problem at the junction with the use of the linearized Lax curves (crosses).

A junction with one ingoing and two outgoing pipes

- The initial data in the pipes are taken as

$$\begin{aligned} w_1 &= (3.4500000,\ 2.4050000,\ 6.5056726); \\ w_2 &= (2.1300000,\ 4.1578000,\ 3.5720977); \\ w_3 &= (2.2534000,\ 2.4191412,\ 2.9335749). \end{aligned} \tag{38}$$

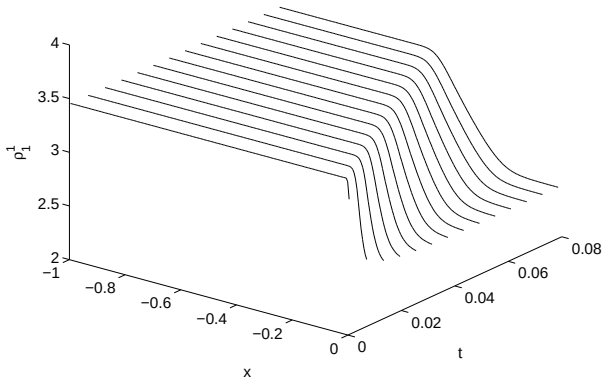

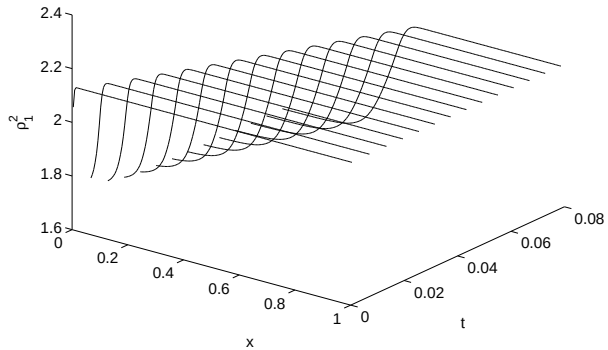

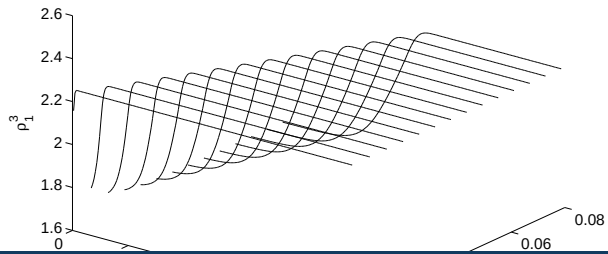

A junction with one ingoing and two outgoing pipes

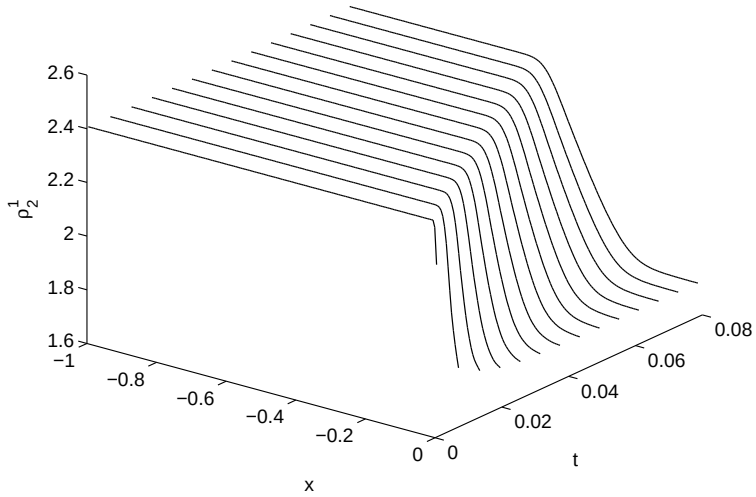

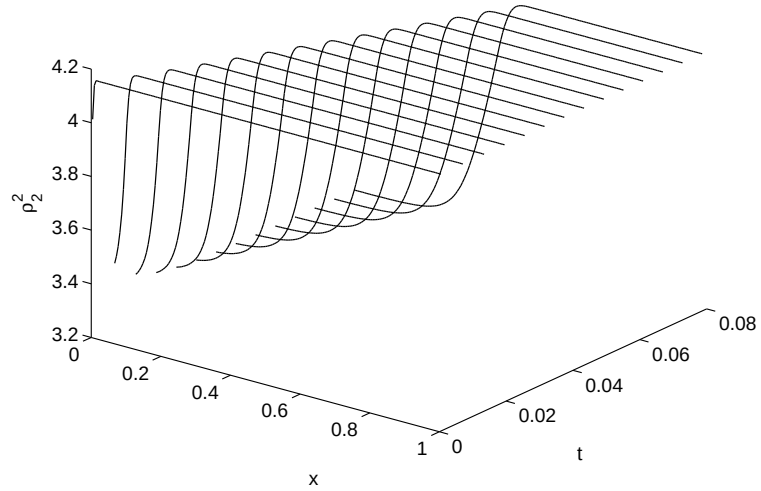

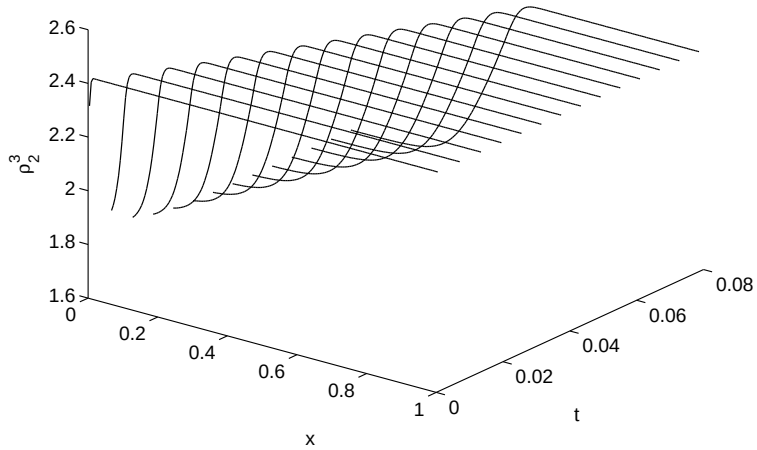

A junction with one ingoing and two outgoing pipes

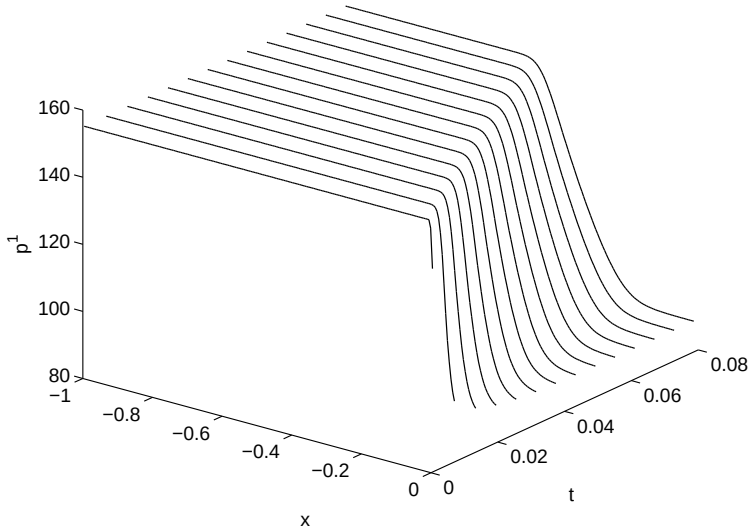

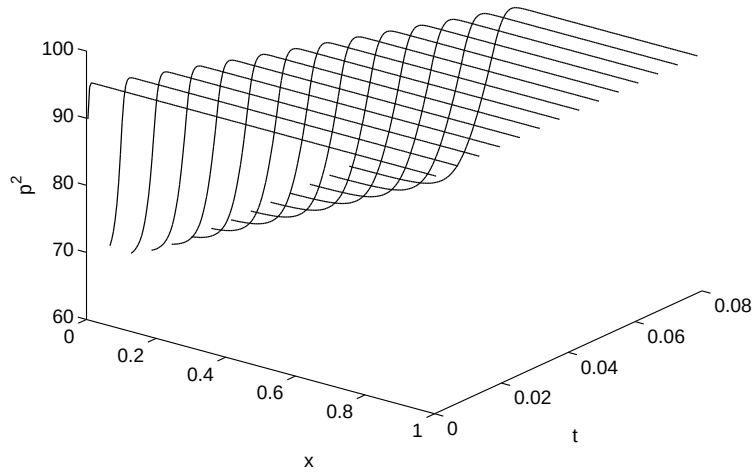

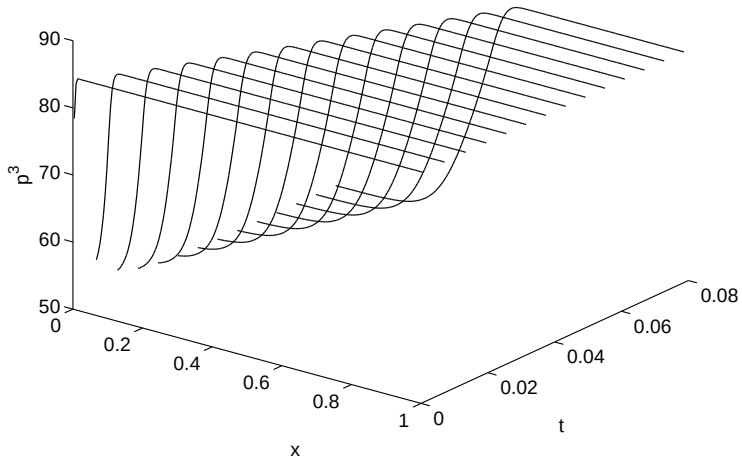

A network of five pipes and two junctions

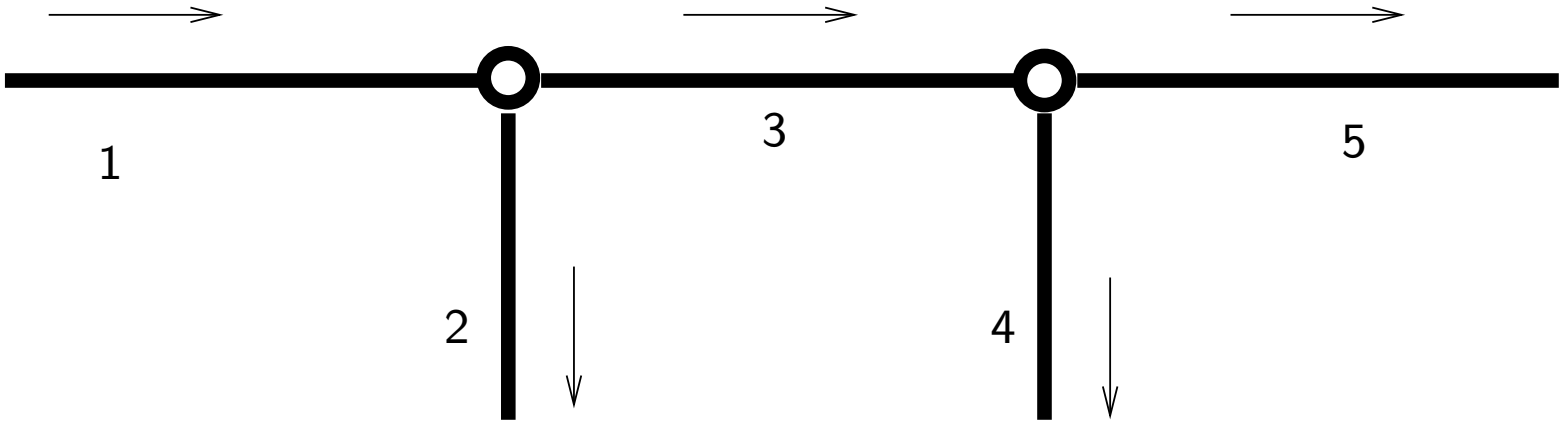

Figure: A small network with two junctions

A network of five pipes and two junctions

- We consider the linear pressure law given by $p = a_1\rho_1 + a_2\rho_2$ with $a_1 = 16$ and $a_2 = 1$. The initial conditions in the pipes are given as

$$
\begin{aligned}
w_1 &= (6.4500, 12.8050, 31.9713);\\
w_2 &= (10.3300, 3.3578, 2.4903);\\
w_3 &= (1.9534, 4.5682, 29.4810);\\
w_4 &= (9.0330, 18.3578, 13.0370);\\
w_5 &= (0.4644, 1.2210, 16.4441).
\end{aligned}
$$

A network of five pipes and two junctions

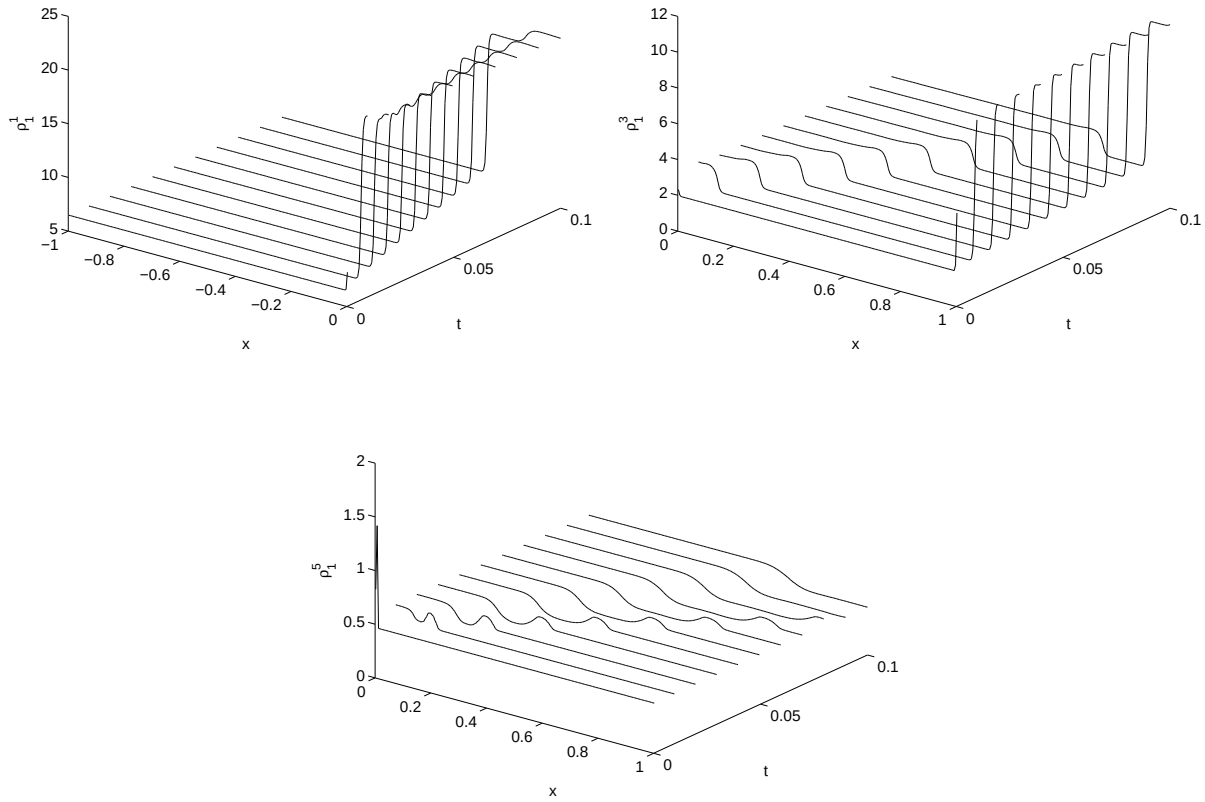

A network of five pipes and two junctions

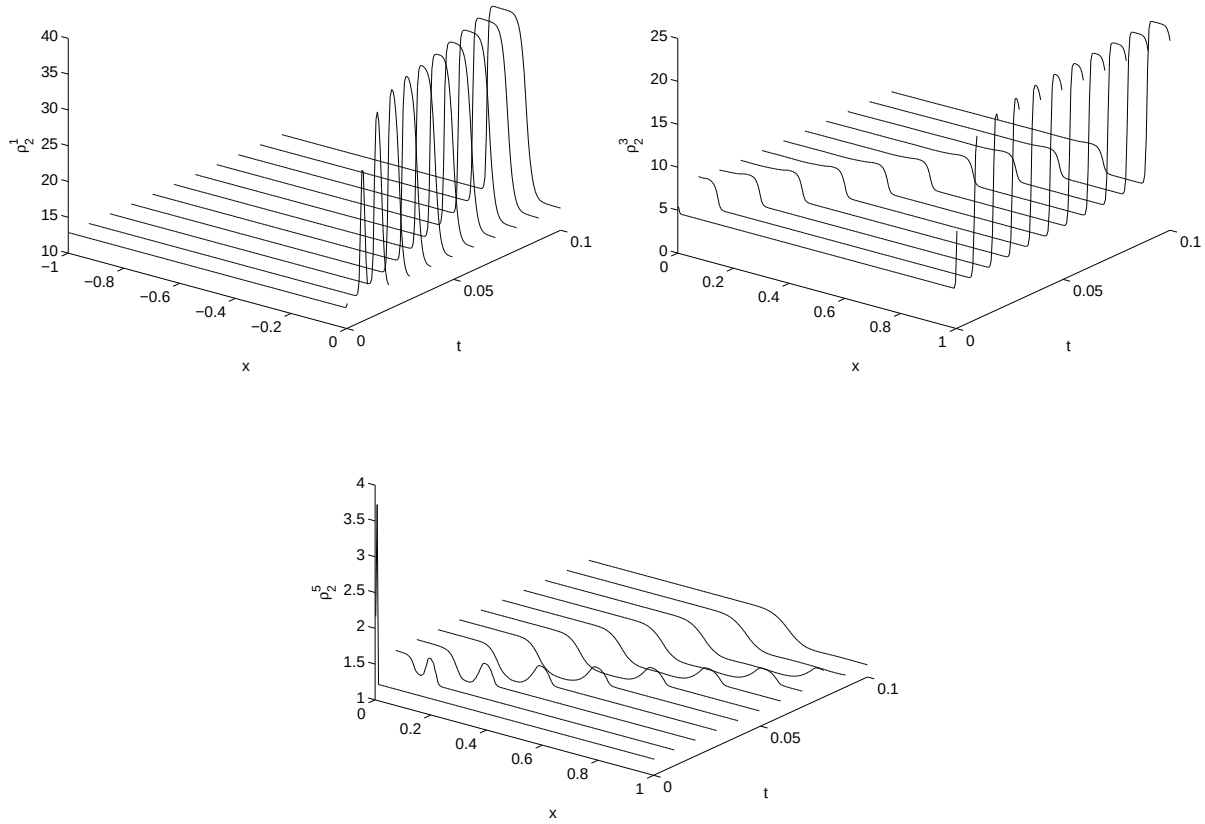

A network of five pipes and two junctions

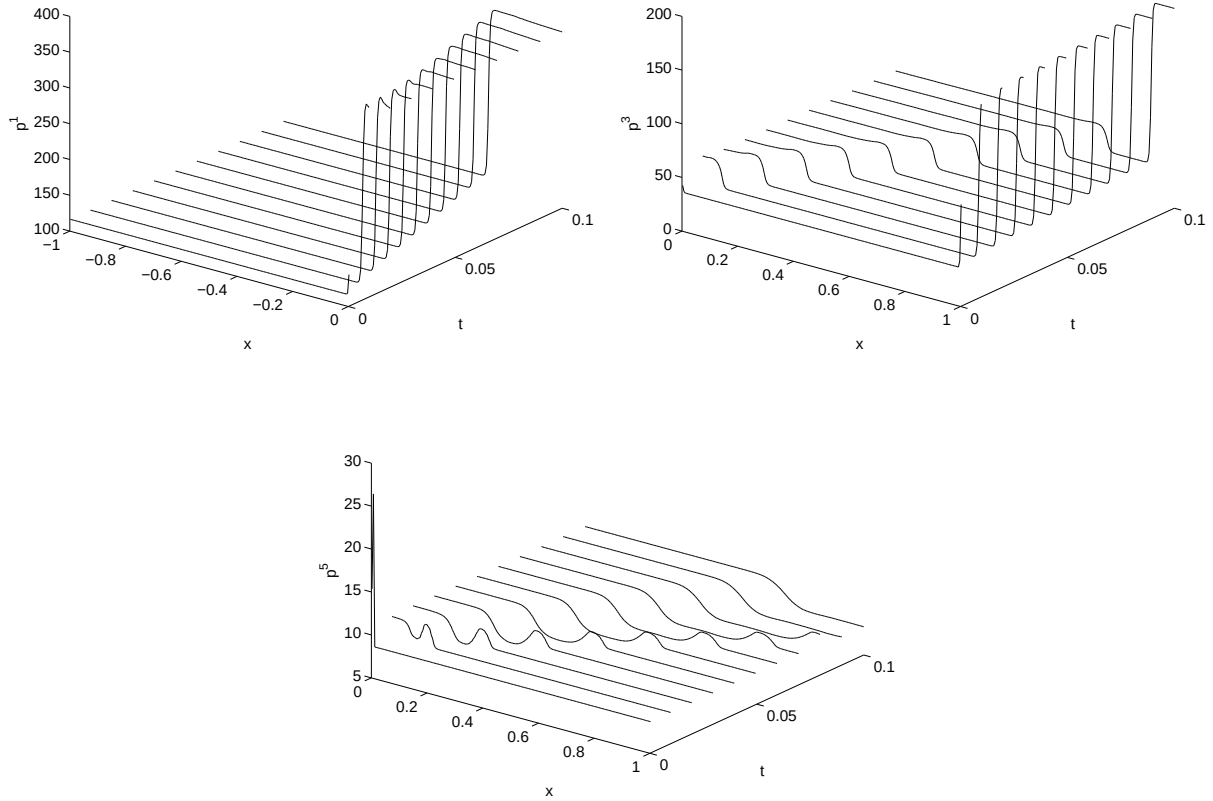

References

Abeysekera, M., J.Wu, N.Jenkins, and M.Rees (2016).

Steady state analysis of gas networks with distributed injection of alternative gas.

Applied Energy, 164:991–1002.

Banda, M. K., Herty, M., and Ngnotchouye, J. M. T. (2010a).

Coupling the drift-flux models with unequal sonic speeds.

Mathematical and Computational Applications, 15(4):574–584.

Banda, M. K., Herty, M., and Ngnotchouye, J. M. T. (2010b).

Towards a mathematical analysis of multiphase drift-flux model in networks.

SIAM J. Sci. Comp, 31(6):4633–4653.

Banda, M. K., Herty, M., and Ngnotchouye, J. M. T. (2015).

On linearized coupling conditions for a class of isentropic multiphase drift-flux models at pipe-to-pipe intersections.

Journal of Computational and Applied Mathematics, 276:81–97.

Bermúdez, A., López, X., and Vázquez-Cendón, M. E. (2017).

Treating network junctions in finite volume solution of transient gas flow models.

Journal of Computational Physics, 344:187–209.

Bressan, A. (2000).

Hyperbolic systems of Conservation laws, volume 20 of *Oxford Lectures Series in Mathematics and its Applications*.

Oxford University Press.

Dafermos, C. M. (2005).

Hyperbolic conservation laws in continum physics, volume 325 of *Grundlehren der mathematischen Wissenschaften*.

Springer, 2 edition.

Domschke, P., Dua, A., Stolwijk, J. J., Langa, J., and Mehrmann, V. (2018).

Adaptive refinement strategies for the simulation of gas flow in networks using a model hierarchy.

Electronic Transactions on Numerical Analysis, 2018.

Accepted.

Dukhovnaya, Y. and Adewumi, M. (2000).

Simulation of non-isothermal transients in gas/condensate pipelines using tvd scheme.

Powder Technology, 112:163–171.

Grimstad, B., Fossa, B., Heddle, R., and Woodman, M. (2016).

Global optimization of multiphase flow networks using spline surrogate models.

Computers and Chemical Engineering, 84:237–254.